

# Thermal Diffusivity Measurement of High-Conductivity Materials by Dynamic Grating Radiometry<sup>1</sup>

Y. Taguchi<sup>2</sup> and Y. Nagasaka<sup>2,3</sup>

---

A new apparatus based on dynamic grating radiometry (DGR) to measure the thermal diffusivity of high-conductivity materials such as graphite and diamond has been developed. In the DGR method, a sample surface is heated by interference of two pulsed laser beams, and the decay of temperature at a spot on the thermal grating is monitored by an infrared detector. In the ideal case where the grating period is much smaller than the light absorption length, the thermal diffusivity parallel to the surface can be determined from the decay constant and the grating period. This paper describes a procedure to extract the thermal diffusivity parallel to the plane while eliminating the effect of anisotropy and gives results for a preliminary measurement using Zr foil. A quadratic dependence of the time constant on fringe space has been observed in the fringe space change. Data are also presented for a 0.1-mm-thick graphite sheet. The results indicate the capability of DGR to measure anisotropic high-conductivity materials.

---

**KEY WORDS:** anisotropic graphite sheet; dynamic grating radiometry; high-conductivity materials; thermal diffusivity.

## 1. INTRODUCTION

Recently, electronic packaging of high-power devices or very densely packed integrated circuits such as ULSI have brought about some serious thermal problems. As one of the ways to solve the problems, high-conductivity materials such as CVD diamond (thermal diffusivity is about  $1000 \text{ mm}^2 \cdot \text{s}^{-1}$ ) have attracted considerable attention and show promise to solve the

---

<sup>1</sup> Paper presented at the Fourteenth Symposium on Thermophysical Properties, June 25–30, 2000, Boulder, Colorado, U.S.A.

<sup>2</sup> Department of Mechanical Engineering, Keio University, 3-14-1, Hiyoshi, Yokohama 223-8522, Japan.

<sup>3</sup> To whom correspondence should be addressed.

problems for heat sinks. In the production process of high-conductivity thin materials, the film will have an anisotropy between directions parallel and directions perpendicular to the plane. However, the study of contact-free thermal diffusivity measurements, which is for anisotropic high-conductivity materials for *in situ* conditions, is not sufficient under existing circumstances. Therefore, a technique for simultaneous measurements of thermal diffusivity parallel and perpendicular to the plane *in situ* is required for the thermal design in a local region.

Graebner [1] developed the transient thermal grating method (TTG), which is a measurement technique for the thermal diffusivity parallel to the plane. In TTG, the thermal diffusivity is detected by the pulsed-laser excitation and thermal radiation detection of a thermal grating on a sample surface. Graebner measured the horizontal thermal properties of CVD diamond films by means of TTG. However, the thermal diffusivity perpendicular to the plane is not considered in TTG. We have adopted the principle of TTG and extended the theory of two-dimensional heat conduction and developed a procedure to analyze the thermal diffusivity parallel to the plane. In the present paper, we discuss the validity of dynamic grating radiometry (DGR) [2, 3] to measure anisotropic thermal diffusivity through a preliminary measurement for Zr foil. According to the results of experimental measurements for graphite sheets, we verify the capability of DGR to measure high-conductivity orthotropic materials.

## 2. PRINCIPLE OF MEASUREMENT

### 2.1. Two-Dimensional Heat Conduction Model

The principle of DGR follows that the transient temperature of the thermal grating is expressed by the heat conduction both parallel and perpendicular to the plane as shown in Fig. 1. If the light absorption length is much larger than the grating period (volume heating), the assumption of one-dimensional heat conduction parallel to the plane ( $x$ -direction) is satisfied (Fig. 1a). On the other hand, if the light absorption length is much smaller than the grating period (surface heating), one-dimensional heat conduction perpendicular to the plane ( $z$ -direction) is permissible in a small area (Fig. 1b). In reality, we need to know the two-dimensional heat conduction process to measure the thermal diffusivity from the infrared signal of the transient temperature decay.

To solve the heat conduction equation, the Green's function [4] as the temperature at  $(x, y, z)$  at point  $(x', y', z')$  at time  $\tau$  is adopted. The Green's function is most conveniently defined for the closed surface as the

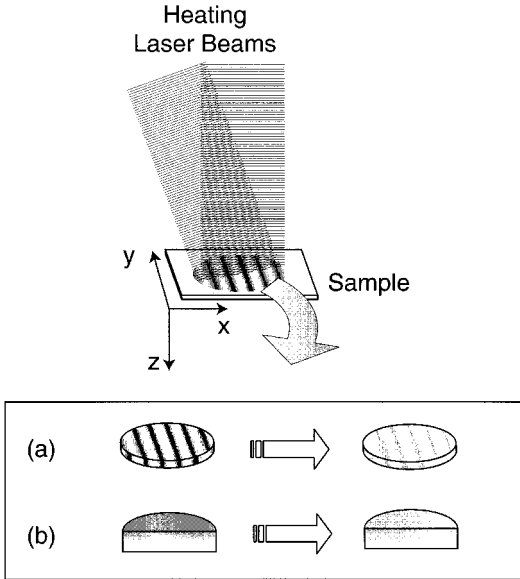


**Fig. 1.** The principle of DGR. (a) Ideal case for one-dimensional heat conduction parallel to the plane. (b) Ideal case for one-dimensional heat conduction perpendicular to the plane.

potential which vanishes over the surface. For any of the boundary conditions, the solution for the two-dimensional region can be expressed as the product of the corresponding one-variable simpler solutions. In this case, the exact shape of the temperature distribution on the  $x$ -axis and  $z$ -axis is described by

$$T_{xz}(x, z, t) = \int G_x \Psi(x') dx' \int G_z \Psi(z') dz' \tag{1}$$

where  $G$  is the Green's function for each direction, and  $\Psi$  is the initial temperature distribution which is excited by heating laser beams. Then each term of Eq. (1) means that

$$T_x(x, t) = \int G_x \Psi(x') dx' \tag{2}$$

$$T_z(z, t) = \int G_z \Psi(z') dz' \tag{3}$$

Equation (2) represents the temperature distribution parallel to the plane, and Eq. (3) represents the temperature distribution perpendicular to the plane. Hence, the two-dimensional heat conduction problem is dealt with for each axis.

The assumptions of one-dimensional heat conduction parallel to the plane are as follows: (1) the sample thickness is semiinfinite ( $-\infty < x < \infty$ ,  $0 < z$ ); (2) there is no inner heat source in the sample; and (3) the grating period  $A$  is much smaller than the laser beam diameter. The initial temperature distribution which is produced by the interference of two laser beams can be written

$$T(x, 0) = T_0 + T_1 \cos(kx) \quad (4)$$

where  $T_0$  is the mean initial temperature rise,  $T_1$  is the spatially periodic temperature distribution, and  $k = 2\pi/A$  is the wave number of the fringe. The solution of the appropriate heat conduction equation is described as follows:

$$T_x(x, t) = T_0 + T_1 \exp\left(-\frac{t}{\tau_x}\right) \cos\left(\frac{2\pi}{A}x\right) \quad (5)$$

where

$$\tau_x = \frac{1}{a_x} \left(\frac{A}{2\pi}\right)^2 \quad (6)$$

$\tau_x$  is the relaxation time of heat conduction, which implies that the spatial temperature distribution decays exponentially. The time decay of the signal is inversely proportional to the thermal diffusivity  $a_x$  and directly proportional to the square of the fringe space  $A^2$ .

In the case of heat conduction for the  $z$ -direction, assumptions of initial states are as follows: (1) the sample is semiinfinite ( $-\infty < x < \infty$ ,  $0 < z < \infty$ ); (2) the surface is heated uniformly; and (3) the sample surface boundaries are adiabatic. By using the initial temperature  $\Psi$ , the temperature at  $z$  at time  $t$  can be written as Eq. (3). In this case of vertical heat conduction, the Green's function  $G_z$  in a sample is given by

$$G_z = \frac{1}{2\sqrt{\pi a_z t}} \left[ \exp\left\{\frac{-(z-z')}{4a_z t}\right\} + \exp\left\{\frac{-(z+z')}{4a_z t}\right\} \right] \quad (7)$$

The initial temperature distribution on the  $z$ -axis  $\Psi(z)$  is given by the following equation:

$$\Psi(z) = \exp(-\alpha z) \quad (8)$$

where  $\alpha$  is the absorption coefficient. The temperature distribution at  $z$  at time  $t$  is given by Eqs. (3), (7), and (8). Then

$$T_z(0, t) = \exp\left(\frac{t}{\tau_z}\right) \operatorname{erfc}\left(\sqrt{\frac{t}{\tau_z}}\right) \quad (9)$$

where  $\tau_z = 1/(a_z \alpha^2)$  is the time constant for the  $z$ -direction,  $a_z$  is the thermal diffusivity perpendicular to the plane, and  $\operatorname{erfc}(x)$  is the complementary error function.

Then, substituting Eqs. (5) and (9) for Eq. (1), the solution of two-dimensional heat conduction applicable to DGR is expressed as follows:

$$T_{xz}(0, 0, t) = \left\{ T_0 + T_1 \exp\left(-\frac{t}{\tau_x}\right) \right\} \left\{ \exp\left(\frac{t}{\tau_z}\right) \operatorname{erfc}\left(\sqrt{\frac{t}{\tau_z}}\right) \right\} \quad (10)$$

As mentioned above, the relative temperature rise which is obtained as Eq. (10) includes the information on two-dimensional heat conduction.

## 2.2. Procedure to Extract $a_x$ from the Two-Dimensional Condition

In real DGR measurement, it is difficult to perform an experiment under the condition of negligible heat flow in the  $z$ -direction. Therefore, in the present study, to analyze the signal which includes information on two-dimensional heat conduction, the thermal diffusivities parallel and perpendicular to the plane are determined separately.

To separate the thermal diffusivities parallel and perpendicular to the plane, the pattern of thermal sinusoidal distribution, which is obtained by scanning the interference pattern on the sample surface, is utilized. Figure 2 shows the temperature distribution on a sample surface heated by an interference pattern. Point A is defined as a peak and point B as a valley of a thermal grating; the temperature distribution of the infrared detector output when the off-axis paraboloidal reflectors spot is located at both extremes is described as

$$T_P(0, 0, t) = \left\{ T_0 + T_1 \exp\left(-\frac{t}{\tau_x}\right) \right\} \left\{ \exp\left(\frac{t}{\tau_z}\right) \operatorname{erfc}\left(\sqrt{\frac{t}{\tau_z}}\right) \right\} \quad (11)$$

$$T_V\left(\frac{A}{2}, 0, t\right) = \left\{ T_0 - T_1 \exp\left(-\frac{t}{\tau_x}\right) \right\} \left\{ \exp\left(\frac{t}{\tau_z}\right) \operatorname{erfc}\left(\sqrt{\frac{t}{\tau_z}}\right) \right\} \quad (12)$$

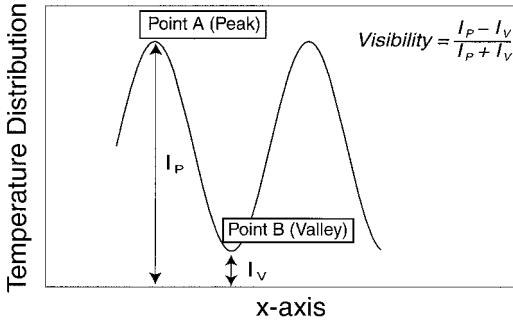


Fig. 2. The ideal temperature distribution of the grating.

where  $T_P$  and  $T_V$  are the temperature decay of the peak and valley, respectively. Then, the heat conduction in the  $z$ -direction is separated by using the peak [Eq. (11)] and valley [Eq. (12)] of thermal grating as follows:

$$T_z = \frac{1}{2} \left\{ T_P(0, 0, t) + T_V\left(\frac{A}{2}, 0, t\right) \right\} = T_0 \exp\left(\frac{t}{\tau_z}\right) \operatorname{erfc}\left(\sqrt{\frac{t}{\tau_z}}\right) \quad (13)$$

Hence, the horizontal temperature distribution  $T_x$  can be expressed as

$$T_x = \frac{T_P}{(T_P + T_V)/2} = 1 + \frac{T_1}{T_0} \exp\left(-\frac{t}{\tau_x}\right) \quad (14)$$

Figure 3, which shows typical data detected by the infrared detector, demonstrates the temperature distribution of points A and B. Using the temperature distribution of the peak and valley, the nondimensional temperature change which includes information on the horizontal thermal diffusivity is determined by Eq. (14). Thus, in DGR, we can obtain the thermal diffusivity parallel to the plane which eliminates the influence of vertical heat conduction problem. By using the simplex method [5], the experimental data can be fitted by Eq. (14) to calculate  $a_x$ .

### 3. EXPERIMENTAL APPARATUS

Figure 4 shows a schematic of the present experimental apparatus. The transient thermal gradient is created by a Nd:YAG laser (wavelength of 532 nm) whose power is  $10 \text{ mJ} \cdot \text{ns}^{-1}$  with a repetition rate of 10-Hz

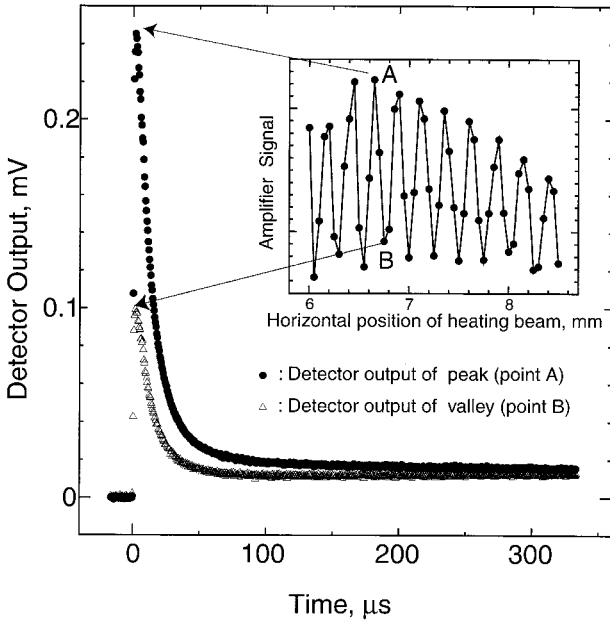


**Fig. 3.** A typical example of two temperature decay outputs when the detection spot is located on a peak and valley with transient thermal grating which is detected by scanning. The sample is 0.05-mm-thick Zr foil.  $\lambda = 332 \mu\text{m}$ .

Q-switch. A pulsed high-power laser beam is divided by a beam splitter into two beams of equal intensity. Two beams are intersected on the sample surface by mirrors under an angle  $\theta$  ( $\theta$  is determined as an interval of M3 and M5) and generate an optical interference fringe pattern whose intensity distribution is spatially sinusoidal. To monitor the decay of temperature distribution which is caused by the heat conduction process, we employ infrared thermometry by measuring the thermal radiation emitted from a spot on the surface. To scan the sample surface, the nano-order moving system which shifts the position of the heated area on the sample is adopted. The off-axis paraboloidal mirrors (the spatial resolving diameter  $\delta$  is estimated to be 100 to 250  $\mu\text{m}$ ) condense the emission from a sample to a  $\text{LN}_2$ -cooled HgCdTe infrared detector (Kolmar Tech., Inc.; KV104-0.05-A-3-SMA), and the weak signal is amplified by a preamplifier (bandwidth of 16 MHz). The detected signal is averaged for a hundred laser pulses to improve the S/N ratio significantly.

Considered as one optical measurement for the anisotropic thermal diffusivity, the characteristics of DGR are summarized as follows: (1) to

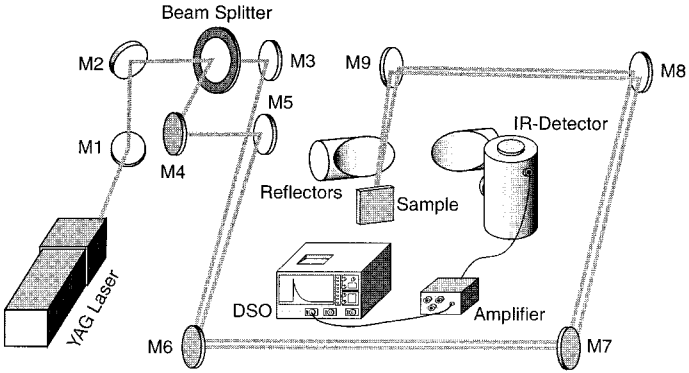


Fig. 4. Experimental apparatus of DGR.

consider two-dimensional heat conduction, the thermal diffusivities parallel and perpendicular to the plane are calculated; (2) quick detection system in DGR can measure the fast decay of surface temperature in high-conductivity materials; (3) the signal is detected by infrared so that DGR can be applied to a sample having not so smooth a surface such as graphite sheet (surface roughness is about  $2\ \mu\text{m}$ ).

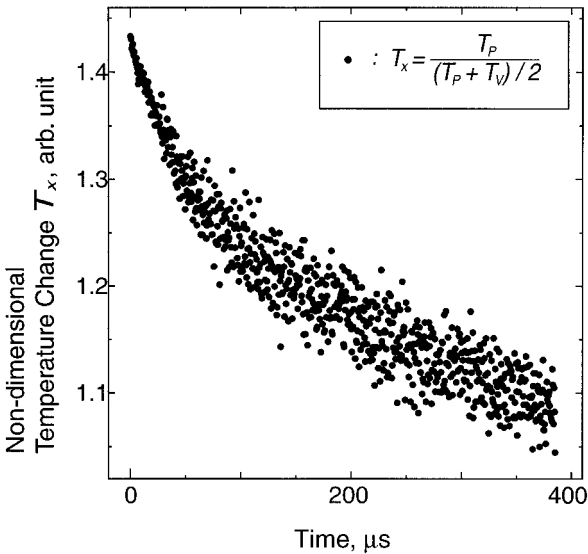


Fig. 5. Nondimensional temperature change  $T_x$  corresponding to the data in Fig. 3.



## 4. RESULTS AND DISCUSSION

### 4.1. Preliminary Measurement Using Zr Foil

To check the validity of the present apparatus and data analysis procedure, we have measured the thermal diffusivity of an isotropic Zr foil of 50- $\mu\text{m}$  thickness. A quadratic dependence of the time constant on the fringe space is observed from 0.261- to 0.464-mm change in the fringe space. Figure 3 shows typical data detected by the infrared detector, and Fig. 5 shows the corresponding derived nondimensional temperature change  $T_x$  from the measurement. As can be seen from Fig. 5, the S/N ratio is inferior due to the nature of the present calculation procedure. This may be improved by redesigning the amplifier or averaging the signal at the digital oscilloscope. Because of the spatial resolving power arising from offset paraboloidal reflectors and the instability of the YAG pulsed beam,  $V_{\text{det}}$  (visibility detected by the infrared detector) is quite frequently smaller than  $V_{\text{CCD}}$  (visibility detected by the CCD camera). Hence, improvement of the S/N ratio requires an increase in the visibility. The quadratic dependence of decay time and fringe space is shown in Fig. 6. The time constant, which

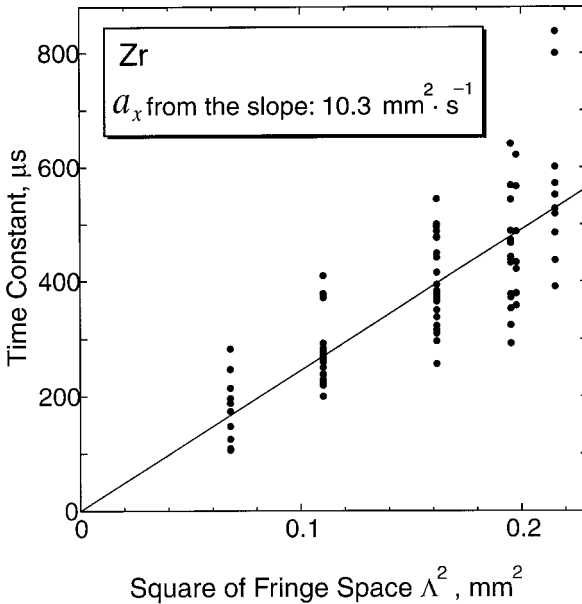


**Fig. 6.** The quadratic dependence of time constant on fringe space. The thermal diffusivity parallel to the plane is calculated as  $10.3 \text{ mm}^2 \cdot \text{s}^{-1}$  from the slope.

**Table I.** Specifications of the Graphite Sheet

Thermal conductivity	$\lambda_{\parallel}$ : 600 to 1000 $\text{W} \cdot \text{m}^{-1} \cdot \text{K}^{-1}$ $\lambda_{\perp}$ : 5 $\text{W} \cdot \text{m}^{-1} \cdot \text{K}^{-1}$
Density	About 1.0 $\text{g} \cdot \text{cm}^{-3}$
Thickness	About 0.1 mm

is calculated by the analysis of the two-dimensional heat conduction model, is proportional to the square of the fringe space. Consequently, the applicability of the principle and the present instrumentation of DGR are confirmed.

#### 4.2. Experiment Using a Graphite Sheet

To confirm the capability of the present DGR apparatus for high-conductivity material, a graphite sheet is studied. The graphite sheet has a high conductivity and anisotropy in directions parallel and perpendicular to the plane (Table I) [6]. For measuring the thermal diffusivity of the graphite sheet, the fringe space is widened to obtain longer decay time constants.

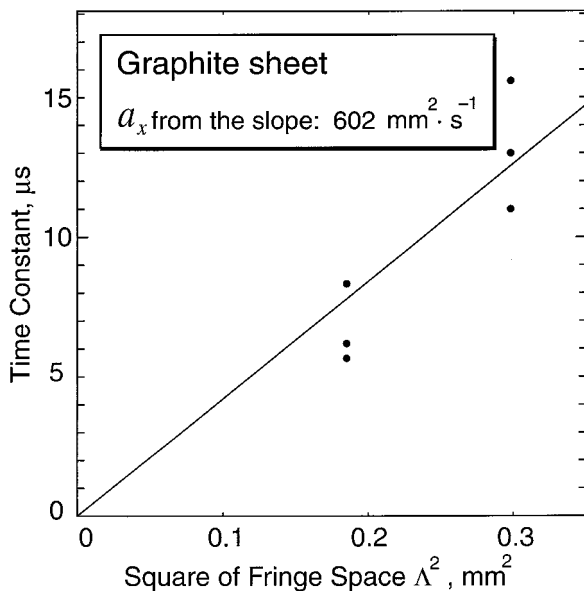


**Fig. 7.** The quadratic dependence of time constant on fringe space. The thermal diffusivity parallel to the plane is calculated as  $602 \text{ mm}^2 \cdot \text{s}^{-1}$  from the slope.

Considering the time dependence on the fringe space, Fig. 7 shows the time constant on each grating ( $A = 545.6$  and  $430.3 \mu\text{m}$ ). The decay time is fitted to a quadratic dependence on the fringe space. The thermal diffusivity of graphite sheet is calculated as  $602 \text{ mm}^2 \cdot \text{s}^{-1}$  by analyzing the slope in Fig. 7. Also, we considered the analysis of anisotropy (Section 2.3). In the experiment on Zr foil, the vertical thermal diffusivity to the plane is impossible to calculate because the heat flow perpendicular to the sample is instantaneous. Compared with horizontal heat conduction, the vertical heat conduction of anisotropic materials such as a graphite sheet is less (Table I). To determine the thermal diffusivity perpendicular to the plane, the absorption length is required. However, the absorption coefficient of graphite sheet is unknown; thus, we assumed a length of  $10^{-6} \text{ m}$ , the value for graphite [7]. Then, as a rough approximation, the thermal diffusivity perpendicular to the plane is estimated to be  $7.9 \text{ mm}^2 \cdot \text{s}^{-1}$ . This leads us to the conclusion that DGR may be suited to measure high-conductivity anisotropic materials such as a graphite sheet.

## ACKNOWLEDGMENT

The work described in this paper was financially supported in part by the Science and Technology Agency under the Promotion System for Intellectual Infrastructure of Research and Development.

## REFERENCES

1. J. E. Graebner, *Rev. Sci. Instrum.* **66**:3903 (1995).
2. T. Ushiku, Y. Taguchi, and Y. Nagasaka, *Proc. 36th Natl. Heat Transfer Symp. Jpn.* (1999), pp. 699–700.
3. Y. Taguchi, and Y. Nagasaka, *Proc. 37th Natl. Heat Transfer Symp. Jpn.* (2000), pp. 903–904.
4. H. S. Carslaw, and J. C. Jaeger, *Conduction of Heat in Solids*, 2nd ed. (Oxford University Press, London, 1959), pp. 353–362.
5. J. A. Nelder, and R. Mead, *Comp. J.* **7**:308 (1965).
6. T. Hoshi, and M. Murakami, *National Technical Report* **40**(1):74–80 (1994).
7. E. D. Palik, *Handbook of Optical Constants of Solids II* (Academic Press, Boston, 1991), pp. 449–460.